The Canadian Mineralogist
Vol. 58, pp. 815-827 (2020)
DOI: 10.3749/canmin.2000007

LIMOUSINITE, $BaCa[Be_4P_4O_{16}]\cdot 6H_2O$, A NEW BERYLLOPHOSPHATE MINERAL WITH A PHILLIPSITE-TYPE FRAMEWORK

FRÉDÉRIC HATERT[§], FABRICE DAL BO, AND YANNICK BRUNI

Laboratoire de Minéralogie, Université de Liège B18, B-4000 Liège, Belgium

NICOLAS MEISSER

Musée de géologie, Université de Lausanne, Quartier Dorigny-Chamberonne, Bâtiment Anthropole, CH-1015 Lausanne, Switzerland

PIETRO VIGNOLA

CNR-Istituto per la Dinamica dei Processi Ambientali, via Mario Bianco, 9 - 20131 Milano, Italia

ANDREA RISPLENDENTE

Dipartimento di Scienze della Terra, Università degli Studi di Milano, via Botticelli 2, 20133 Milano, Italia

FRANÇOIS-XAVIER CHÂTENET

Chemin du Gorceix 7, F-87510 Saint-Jouvent, France

JULIEN LEBOCEY

Rue Guingouin 46, F-87410 Le-Palais-sur-Vienne, France

ABSTRACT

Limousinite, ideally $BaCa[Be_4P_4O_{16}]\cdot 6H_2O$, is a new beryllophosphate mineral discovered in the Vilatte-Haute pegmatite, Chanteloube near Razès, Limousin, Haute-Vienne, France. The new mineral is intimately associated with microcrystalline pale brown greifensteinite, black amorphous vitreous Mn-oxyhydroxide, triplite, and quartz. It forms isolated, partly corroded, colorless to snow-white crystals up to 0.9 mm long, showing rhombic cross sections. Limousinite is transparent with a vitreous luster, non-fluorescent, without cleavage planes; its calculated density is 2.58 g/cm^3. Optically, the mineral is biaxial negative, $\alpha = 1.532(2)$, $\beta = 1.553(3)$, $\gamma = 1.558(2)$ (measured under 589 nm wavelength light), $2V_{calc.} = 18°$, non-dispersive, with Z parallel to the elongation of the prismatic crystals. Electron-microprobe analyses indicate an empirical formula of $(Ba_{0.91}K_{0.07})_{\Sigma 0.98}(Ca_{0.87}Na_{0.05})_{\Sigma 0.92}[(Be_{3.87}Al_{0.13})_{\Sigma 4}P_4O_{16}]\cdot 5.56H_2O$, calculated on the basis of 4 P atoms per formula unit, assuming 4 (Be + Al) *pfu* and a water content calculated from refined site-occupancy factors. A single-crystal structure refinement was performed to $R_1 = 4.90\%$, in the $P2_1/c$ space group, with $a = 9.4958(4)$, $b = 13.6758(4)$, $c = 13.4696(4)$ Å, $\beta = 90.398(3)°$, $V = 1749.15(10)$ Å^3, $Z = 4$. The crystal structure is characterized by a beryllophosphate framework similar to that of phillipsite-group zeolites, based on corner-sharing BeO_4 and PO_4 tetrahedra forming interconnected four- and eight-membered rings. Large cages within this zeolite framework contain Ba, Ca, and water molecules. Limousinite is the third known natural zeolite-type beryllophosphate, together with pahasapaite and wilancookite; it is also the first phosphate with a framework identical to that of a natural zeolite silicate.

Keywords: limousinite, beryllophosphate, new mineral, zeolite, phillipsite framework, Chanteloube, Limousin, France.

§ *Corresponding author e-mail address*: fhatert@uliege.be

Introduction

The Limousin region, France, is extremely rich from a geological point of view. Indeed, more than 60 granitic pegmatites occur in this region, particularly in the Ambazac Mountains, Haute-Vienne. These pegmatites were mined in the 19th century and at the beginning of the 20th century, mainly for feldspar and kaolin used in the nearby Limoges porcelain factories.

From a mineralogical point of view, these pegmatites contain Fe-Mn-bearing phosphate minerals which have been investigated by famous mineralogists such as Alexis Damour, François II Alluaud, and N. Vauquelin. Four mineral species have their type localities in this region: alluaudite (Damour 1847, 1848, Moore & Ito 1979, Hatert 2019), heterosite and hureaulite (Alluaud 1826), and triplite (Vauquelin 1802, Hausmann 1813).

Recent field investigations resulted in the discovery of new phosphate samples in the Villatte-Haute quarry at Chanteloube. Among these samples of primary Fe-Mn phosphates, alteration vugs were found, containing colorless prismatic crystals which appeared to be a new Ba-bearing phosphate. A complete structural characterization indicated that this mineral is a new barium beryllophosphate, structurally related to the phillipsite group of zeolites. The species was submitted to the IMA-CNMNC under number IMA 2019-011, and was approved by this commission.

This phosphate was named limousinite, for the French historical region *Limousin* from which it was collected. The name *Limousin* is derived from *Lemovices*, a native first millenary BC Gaulish tribe; *Lemovices* stems from *lemo* "elm" and *vices* "who win" or evidently: "winners with elm" (Delamarre 2003). This name is also well known as a race of cattle and as a style of coach-built cars.

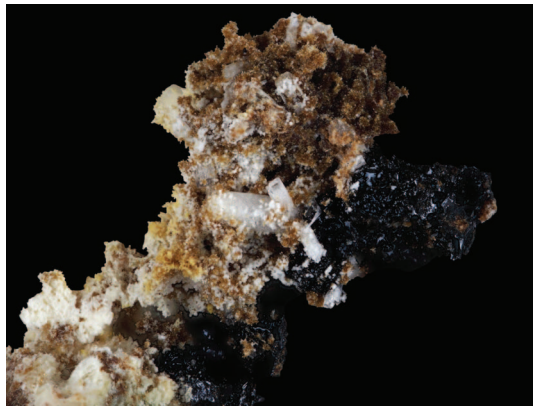

FIG. 1. Prismatic, colorless crystals of limousinite associated with microcrystalline pale brown greifensteinite and black amorphous vitreous Mn-oxyhydroxides. FOV: 1 mm.

Parts of the type sample are deposited in the Geological Museum of Lausanne, Switzerland (X-ray powder pattern: catalogue number: MGL n°093398), and in the Laboratory of Mineralogy of the University of Liège, Belgium (optics, crystal structure determination, electron-microprobe data: catalogue number ULG 21167). A detailed mineralogical characterization of this new species is given in the present paper.

Occurrence

The new barium beryllophosphate mineral limousinite occurs at the historical pegmatite phosphate locality of Vilatte-Haute quarry, Chanteloube near

TABLE 1. CHEMICAL DATA FOR LIMOUSINITE

Constituent	Mean wt.%	Range	Stand. Dev.	Cation	Cation numbers (B = 4 P)
P_2O_5	42.06	38.68–44.64	2.10	P	4.000
SiO_2	0.02	0.00–0.04	0.01	Si	0.002
Al_2O_3	0.99	0.84–1.15	0.13	Al	0.131
MgO	0.02	0.00–0.04	0.02	Mg	0.004
ZnO	0.03	0.00–0.11	0.04	Zn	0.000
FeO	0.02	0.00–0.08	0.02	Fe^{2+}	0.002
CaO	7.20	6.96–7.43	0.15	Ca	0.867
BaO	20.60	19.78–21.56	0.51	Ba	0.907
SrO	0.06	0.00–0.18	0.07	Sr	0.004
Na_2O	0.21	0.11–0.27	0.05	Na	0.047
K_2O	0.47	0.35–0.57	0.06	K	0.068
BeO*	14.34	-	-	Be	3.869
H_2O*	14.83	-	-	H	11.120
Total	100.85				

* Calculated from the crystal-structure data.

TABLE 2. X-RAY POWDER DIFFRACTION PATTERN OF LIMOUSINITE (d in Å)

$I_{obs.}$	$d_{obs.}$	$I_{calc.}$	$d_{calc.}$	hkl
20	7.80	80	7.809	1 1 0
20	6.78	42	6.838	0 2 0
30	6.05	100	6.101	0 2 1
10	4.10	56	4.111	1 3 0
100	**3.89**	76	3.902	1 1 $\bar{3}$
60	**3.75**	50	3.749	2 2 1
10	3.51	20	3.513	1 3 $\bar{2}$
60	**3.09**	30	3.100	1 1 $\bar{4}$
90	**3.01**	46	3.010	3 1 1
20	2.95	25	2.952	2 2 $\bar{3}$
20	2.81	15	2.807	3 1 2
10	2.61	23	2.610	1 3 $\bar{4}$
30	2.58	35	2.580	1 5 1
10	2.56	13	2.569	2 4 $\bar{2}$
30	2.430	24	2.430	3 3 $\bar{2}$
5	2.371	7	2.378	4 0 0
20	2.276	8	2.280	0 6 0
50	**2.219**	8	2.223	2 2 $\bar{5}$
20	2.149	9	2.145	2 4 $\bar{4}$
60	**2.058**	19	2.063	3 3 $\bar{4}$
20	1.971	14	1.967	2 6 $\bar{2}$
40	**1.879**	7	1.884	5 1 0
5	1.759	3	1.756	2 6 $\bar{4}$
40	**1.735**	5	1.737	5 1 3
10	1.649	1	1.647	5 1 $\bar{4}$
20	1.645	8	1.646	4 6 0
20	1.603	6	1.602	0 6 6
5	1.590	7	1.585	6 0 0
20	1.556	4	1.555	1 5 7

Data collected with a Gandolfi camera, 114.6 mm diameter, Ni-filtered Cu$K\alpha$ radiation ($\lambda = 1.5418$ Å), Si as external standard. Intensities were estimated visually. Calculated intensities were obtained from the structural data with POWDER CELL (Krauz & Nolze 1996). Calculated d values were refined with LCLSQ (Burnham 1991); the refined unit-cell parameters are: $a = 9.512(7)$, $b = 13.677(14)$, $c = 13.503(18)$ Å, $\beta = 90.10(10)°$ (space group $P2_1/c$).

TABLE 3. EXPERIMENTAL DETAILS FOR THE SINGLE-CRYSTAL X-RAY DIFFRACTION STUDY OF LIMOUSINITE

Ideal structural formula	$BaCa[Be_4P_4O_{16}]\cdot 6H_2O$
a (Å)	9.4958(4)
b (Å)	13.6758(4)
c (Å)	13.4696(4)
β (°)	90.398(3)
V (Å^3)	1749.15(10)
Space group	$P2_1/c$
Z	4
D_{calc} (g.cm^{-3})	2.664
Absorption coefficient (mm^{-1})	3.046
F(000)	1360
Radiation	Mo$K\alpha$, 0.71073
Crystal size (mm)	0.097 × 0.098 × 0.139
Color and habit	Colorless prismatic
Temperature (K)	293(2)
θ range (°)	2.60–28.65
Reflection range	$-11 \le h \le 12$, $-17 \le k \le 11$, $-18 \le l \le 16$
Total no. of reflections	13429
Unique reflections	4090
Refined parameters	355
R_1, $F^2 > 2\sigma(F^2)$	0.0490
R_1, all data	0.0713
wR_2 (F^2), all data	0.1104
GOF	1.063
$\Delta\sigma_{min}$, $\Delta\sigma_{max}$ (e/Å^3)	–1.122, 1.158

Razès, Limousin, Haute-Vienne, France. The geographical coordinates of the locality are 46.066° N/01.367° E.

Primary nodular Li-Mn-Fe-phosphates (mostly triplite, alluaudite, and heterosite) embedded in the Chanteloube beryl-bearing pegmatite are locally associated with pyrite and löllingite. Within these minerals, supergene alteration created dissolution vugs containing free-grown microminerals, including numerous secondary phosphates and arsenates: arthurite, bendadaite, beraunite, cacoxenite, dufrénite, fluellite, frondelite, goudeyite, greifensteinite, hureaulite, jahnsite-(CaMnFe), leucophosphite, metazeunerite, olivenite, pharmacosiderite, phosphosiderite, rittmannite, scorodite, stewartite, strengite, symplesite, whitmoreite, the new Mn equivalent of bendadaite, and the (FeFeFe)-equivalent of whiteite (Meisser *et al*. 2009, Lebocey *et al*. 2010, Meisser 2010).

Limousinite was discovered in these alteration vugs, in close association with microcrystalline pale brown greifensteinite, black amorphous vitreous Mn-oxyhydroxide, and earlier triplite and quartz. The mineral was probably formed by acid leaching (from arsenopyrite and löllingite alteration) of fluorapatite and beryl and subsequently crystallized in vugs. The Ba source remains unknown.

Physical and Optical Properties

Limousinite forms isolated, partly corroded, colorless to snow-white prismatic crystals up to 0.9 mm long (Fig. 1) with rhombic cross sections. The mineral is transparent with a vitreous luster, it is non-fluorescent, and brittle without cleavage planes. The density has not been measured due to the small size of the crystals, but the calculated density, obtained from

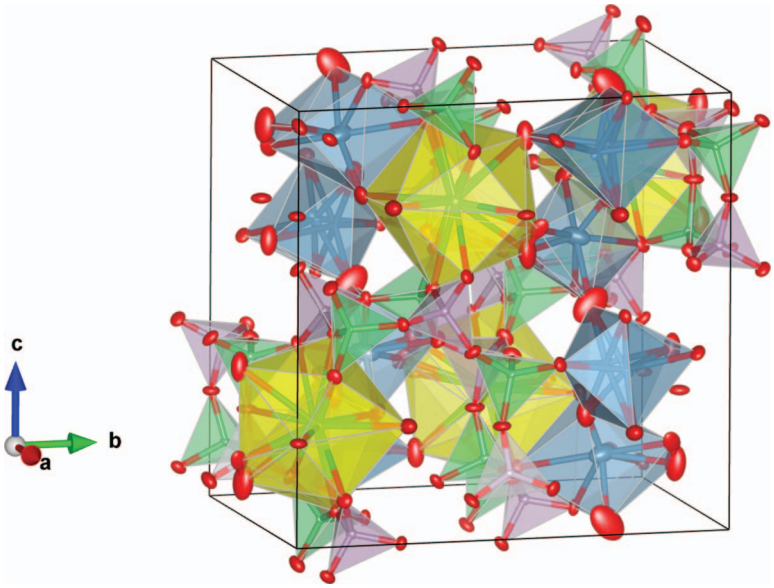

FIG. 2. The crystal structure of limousinite. PO_4 polyhedra are violet, BeO_4 are green, CaO_8 are blue, and BaO_{13} are yellow.

the empirical formula and the single-crystal unit-cell parameters, is 2.58 g/cm^3.

Under the polarizing microscope, limousinite is colorless and non-pleochroic, biaxial negative, with $\alpha = 1.532(2)$, $\beta = 1.553(3)$, $\gamma = 1.558(2)$ (measured under 589 nm wavelength light). The $2V$ angle has not been measured, but the calculated $2V$ is 18°, and the mineral is non-dispersive. The optical orientation has not been completely determined, but Z is parallel to the elongation of the prisms.

CHEMICAL COMPOSITION

Chemical data for limousinite (Table 1) were obtained with a Jeol JXA-8200 electron microprobe working in WDS mode in the Department of Earth Sciences, University of Milan, Italy. The acceleration voltage was 15 kV, beam current 5 nA, and beam diameter 1 μm. The standards used were graftonite from Kabira, Uganda (KF-16, Fransolet 1975), for Fe, Ca, and P, andradite for Si, anorthite (An137) for Al, forsterite (US NM2566) for Mg, willemite for Zn, baryte for Ba, celestine for Sr, omphacite (US NM110607) for Na, and orthoclase (PSU OR 1A) for K. H_2O, CO_2, and BeO were not determined due to the small grain size, but the ideal H_2O and BeO contents were calculated according to the structural data.

A total of 15 point analyses were obtained, leading to the empirical formula $(Ba_{0.91}K_{0.07})_{\Sigma 0.98}(Ca_{0.87}Na_{0.05})_{\Sigma 0.92}[(Be_{3.87}Al_{0.13})_{\Sigma 4}P_4O_{16}]\cdot 5.56H_2O$, calculated on the basis of 4 P atoms per formula unit, assuming 4 (Be + Al) *pfu* and a water content calculated from refined site-occupancy factors (Table 1). The simplified formula is $(Ba,K)(Ca,Na)[(Be,Al)_4\ P_4O_{16}]\cdot 6H_2O$, and the ideal formula is $BaCa[Be_4\ P_4O_{16}]\cdot 6H_2O$, which requires P_2O_5 40.47, CaO 7.99, BaO 21.86, BeO 14.26, H_2O 15.41, total 100 wt.%. The Gladstone-Dale compatibility index for limousinite, 1 – (Kp/Kc), is equal to –0.033, so the compatibility of this new species is excellent, according to Mandarino (1981).

X-RAY DIFFRACTION

X-ray powder diffraction data (Table 2) were collected with a 114.6 mm diameter Gandolfi camera, using Cu$K\alpha$ radiation, with $\lambda = 1.5418$ Å. Unit-cell parameters were refined from the powder diffraction data using the LCLSQ software (Burnham 1991): $a = 9.512(7)$, $b = 13.677(14)$, $c = 13.503(18)$ Å, $\beta = 90.10(10)°$, $V = 1757(2)$ Å^3, $Z = 4$, space group $P2_1/c$ (inferred from single-crystal data).

The X-ray structural study was carried out with a crystal of limousinite measuring 0.097 × 0.098 × 0.139 mm and a Rigaku Xcalibur 4-circle diffractometer equipped with an EOS detector and Mo$K\alpha$ radiation ($\lambda = 0.71073$ Å). A total of 387 frames with a spatial resolution of 1° were collected by the φ/ω scan technique, with a counting time of 20 s per frame, in the range $5.20° < 2\theta < 57.30°$. A total of 13,429 reflections were extracted from these frames, corresponding to 4090 unique reflections. The unit-cell parameters refined from these reflections are in fairly

TABLE 4. ATOM COORDINATES AND ISOTROPIC DISPLACEMENT PARAMETERS (Å^2) FOR LIMOUSINITE

	x	*y*	*z*	U_{eq}
Ba[1]	0.7855(12)	0.0933(3)	0.2512(3)	0.0227(11)
Ba1[2]	0.7353(2)	0.09312(4)	0.25000(3)	0.0185(3)
Ca[3]	1.1555(18)	0.2448(16)	0.1268(9)	0.003(4)
Ca1[4]	1.1191(3)	0.2845(3)	0.13907(18)	0.0185(10)
Ca2[5]	1.3786(7)	0.2817(5)	0.3622(4)	0.064(2)
P1	0.91470(14)	0.14375(10)	0.01714(9)	0.0133(3)
P2	0.58680(14)	0.14477(10)	0.48613(9)	0.0134(3)
P3	0.41003(14)	0.01095(10)	0.13990(9)	0.0158(3)
P4	1.08646(14)	0.01036(10)	0.35971(9)	0.0139(3)
Be1	0.5986(6)	0.1381(5)	0.0141(4)	0.0096(12)
Be2	0.9025(7)	0.1404(4)	0.4837(4)	0.0089(12)
Be3	1.1036(7)	0.0157(5)	0.1353(5)	0.0123(12)
Be4	0.3950(7)	0.0153(5)	0.3650(5)	0.0143(13)
O1	0.9788(4)	0.0892(3)	0.3860(3)	0.0214(8)
O2	1.0035(4)	0.1092(3)	0.1057(3)	0.0230(9)
O3	0.5635(4)	0.0880(3)	0.5827(3)	0.0237(9)
O4	0.9613(4)	0.2493(3)	–0.0033(3)	0.0195(8)
O5	0.7396(4)	0.1391(3)	0.4524(3)	0.0193(8)
O6	0.5406(4)	0.2498(3)	0.5037(3)	0.0197(8)
O7	0.4973(4)	0.1033(3)	0.4019(3)	0.0266(9)
O8	0.7612(4)	0.1396(3)	0.0495(3)	0.0195(8)
O9	0.9423(4)	0.0833(3)	–0.0755(3)	0.0232(9)
O10	1.0512(4)	–0.0852(3)	0.4142(3)	0.0252(9)
O11	0.5189(4)	0.0846(3)	0.1050(3)	0.0260(9)
O12	0.4329(5)	–0.0888(3)	0.0917(3)	0.0330(10)
O13	1.0730(4)	–0.0116(3)	0.2497(3)	0.0250(9)
O14	1.2336(4)	0.0466(3)	0.3880(3)	0.0221(9)
O15	0.2630(4)	0.0497(3)	0.1145(3)	0.0265(9)
O16	0.4336(4)	–0.0017(3)	0.2510(3)	0.0283(10)
OW1A[6]	0.805(3)	–0.094(2)	0.181(2)	0.037(8)
OW1B[7]	0.766(2)	–0.0772(10)	0.127(3)	0.071(8)
OW2[8]	0.5776(6)	0.2694(4)	0.2470(4)	0.045(2)
OW3[9]	0.9410(6)	0.2682(4)	0.2610(4)	0.0416(19)
OW4[10]	1.2608(7)	0.2293(8)	0.0057(7)	0.094(4)
OW5[11]	0.7270(6)	–0.0791(4)	0.3863(5)	0.050(2)
OW6[12]	1.2815(7)	0.2251(5)	0.2562(5)	0.059(3)
HW1	0.821(10)	–0.097(7)	0.110(8)	0.04(4)
HW2A	0.4890(17)	0.263(3)	0.236(5)	0.06(1)
HW2B	0.604(4)	0.314(2)	0.207(3)	0.01(1)
H1A	0.692(5)	–0.096(4)	0.318(4)	0.01(1)
H1B	0.863(2)	0.288(3)	0.236(3)	0.01(1)
H1C	0.923(4)	0.250(3)	0.3200(13)	0.02(2)
H1D	1.230(6)	0.289(4)	–0.016(4)	0.01(1)
H1E	1.177(6)	0.232(4)	0.239(3)	0.01(1)

Occupancies: 1 = 0.137(7) Ba, 2 = 0.809(8) Ba, 3 = 0.077(9) Ca, 4 = 0.545(9) Ca, 5 = 0.332(6) Ca, 6 = 0.40(6) O, 7 = 0.61(6) O, 8 = 0.943(14) O, 9 = 0.932(14) O, 10 = 0.89(2) O, 11 = 0.908(17) O, 12 = 0.876(18) O.

good agreement with those refined from the X-ray powder data (see above). Data were corrected for Lorentz, polarization, and absorption effects, the latter by using an empirical method and the SCALE3 ABSPACK scaling algorithm included in the CrysAlisRED package (Oxford Diffraction 2007). Further details on the structure solution and refinement are given in Table 3.

The crystal structure of limousinite (Fig. 2) was refined in space group $P2_1/c$, with $a = 9.4958(4)$, $b = 13.6758(4)$, $c = 13.4696(4)$ Å, $\beta = 90.398(3)°$, $V = 1749.15(10)$ Å^3, and $Z = 4$. Scattering curves for

TABLE 5. ANISOTROPIC DISPLACEMENT PARAMETERS (Å^2) FOR LIMOUSINITE

	U_{11}	U_{22}	U_{33}	U_{23}	U_{13}	U_{12}
Ba1	0.0206(7)	0.0212(2)	0.0138(2)	–0.00082(17)	–0.00237(18)	0.0004(2)
Ca1	0.0083(12)	0.0226(19)	0.0245(12)	0.0079(10)	–0.0035(8)	–0.0038(12)
Ca2	0.074(4)	0.079(5)	0.038(3)	–0.013(3)	0.002(2)	0.015(3)
P1	0.0164(7)	0.0112(7)	0.0123(7)	–0.0005(5)	0.0018(5)	0.0001(5)
P2	0.0145(7)	0.0115(7)	0.0143(7)	0.0009(5)	0.0014(5)	–0.0008(5)
P3	0.0187(7)	0.0182(7)	0.0104(7)	–0.0002(5)	0.0006(5)	–0.0044(5)
P4	0.0165(7)	0.0149(7)	0.0101(7)	0.0002(5)	0.0009(5)	0.0025(5)
Be1	0.006(3)	0.013(3)	0.009(3)	0.000(2)	–0.002(2)	–0.002(2)
Be2	0.015(3)	0.004(3)	0.007(3)	0.001(2)	0.001(2)	0.001(2)
Be3	0.018(3)	0.010(3)	0.009(3)	–0.002(2)	0.000(2)	0.000(2)
Be4	0.014(3)	0.017(3)	0.012(3)	–0.001(2)	0.002(2)	–0.003(3)
O1	0.019(2)	0.020(2)	0.025(2)	–0.0039(16)	0.0033(14)	0.0059(17)
O2	0.026(2)	0.020(2)	0.022(2)	0.0026(16)	–0.0029(15)	0.0074(17)
O3	0.025(2)	0.022(2)	0.024(2)	0.0114(17)	0.0057(15)	0.0042(18)
O4	0.023(2)	0.014(2)	0.021(2)	0.0022(15)	0.0011(14)	–0.0022(16)
O5	0.0151(19)	0.027(2)	0.0159(19)	–0.0029(15)	0.0032(14)	–0.0004(16)
O6	0.0169(19)	0.013(2)	0.029(2)	–0.0009(15)	0.0024(15)	0.0013(15)
O7	0.023(2)	0.026(2)	0.030(2)	–0.0075(18)	–0.0039(16)	–0.0084(18)
O8	0.017(2)	0.020(2)	0.021(2)	–0.0017(15)	0.0023(14)	–0.0031(16)
O9	0.026(2)	0.025(2)	0.019(2)	–0.0082(16)	0.0043(15)	–0.0037(18)
O10	0.034(2)	0.022(2)	0.019(2)	0.0079(17)	–0.0071(15)	–0.0014(19)
O11	0.018(2)	0.028(2)	0.032(2)	0.0106(18)	0.0032(15)	–0.0038(18)
O12	0.051(3)	0.022(2)	0.026(2)	–0.0067(18)	–0.0080(18)	0.001(2)
O13	0.034(2)	0.031(2)	0.0104(19)	–0.0013(16)	0.0021(15)	–0.0025(19)
O14	0.017(2)	0.027(2)	0.022(2)	–0.0037(16)	–0.0020(14)	0.0014(17)
O15	0.018(2)	0.033(2)	0.029(2)	0.0051(18)	–0.0014(15)	–0.0047(18)
O16	0.033(2)	0.041(3)	0.011(2)	–0.0003(17)	0.0018(16)	0.004(2)
OW1A	0.024(10)	0.038(10)	0.049(14)	–0.012(8)	0.022(8)	–0.014(7)
OW1B	0.047(9)	0.037(7)	0.13(2)	0.008(8)	0.005(11)	0.009(6)
OW2	0.075(5)	0.022(3)	0.039(3)	0.010(2)	0.016(3)	0.007(3)
OW3	0.071(4)	0.028(3)	0.026(3)	0.000(2)	0.007(2)	0.002(3)
OW4	0.030(4)	0.123(10)	0.129(8)	–0.048(7)	–0.004(4)	–0.004(5)
OW5	0.028(3)	0.030(4)	0.091(6)	0.003(3)	–0.003(3)	–0.002(2)
OW6	0.058(5)	0.042(4)	0.076(5)	0.002(3)	0.003(4)	0.013(3)

The Ba and Ca sites were refined isotropically.

neutral atoms, together with anomalous dispersion corrections, were taken from the *International Tables for X-Ray Crystallography, Vol. C* (Wilson 1992). In the final refinement cycle, all atoms except hydrogen and the low-occupancy Ca and Ba sites were refined anisotropically (Tables 4, 5), leading to an R_1 value of 0.0490.

The crystal structure is characterized by a beryllophosphate framework similar to that of phillipsite-group zeolites (Fig. 3). This framework is based on corner-sharing BeO_4 and PO_4 tetrahedra forming interconnected four- and eight-membered rings. Large cages within this zeolite framework contain Ba, Ca, and water molecules. Calcium is distributed over the two Ca1 and Ca2 positions, but the Ca1 site was further split into two close positions, thus leading to final occupancies of 0.077(9) for Ca, 0.545(9) for Ca1, and 0.332(6) for Ca2. In the difference-Fourier maps, significant residual electron densities also appeared close to the Ba1 atom, which was then split into Ba and Ba1, with occupancy factors of 0.137(7) and 0.809(8), respectively (Table 4). Occupancies were refined for the six oxygen atoms, OW1 to OW6, involved in water molecules, leading to a total of 5.56 H_2O molecules *pfu*. Examination of difference-Fourier maps allowed us to localize four H atoms involved in the OW2 and OW3 water molecules, as well as four H atoms involved in the OW1, OW4, OW5, and OW6 water molecules. The OW1 atoms showed an extremely anisotropic displacement ellipsoid; it was consequently decided to split this atom into the two

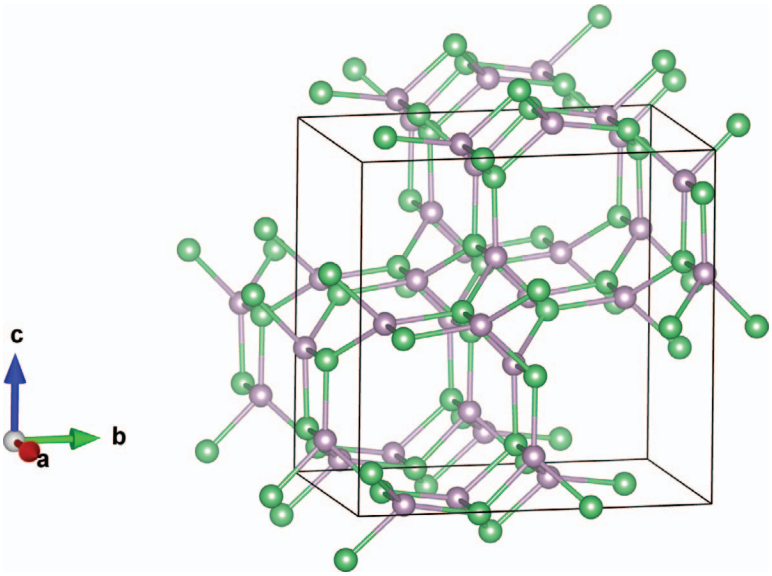

FIG. 3. The framework of limousinite, with Be atoms in green and P atoms in violet. This framework is identical to that of phillipsite-group zeolites, with a combination of four-membered rings and eight-membered rings.

positions OW1A [*s.o.f.* 0.45(9)] and OW1B [*s.o.f.* 0.60(9)].

Ba/Ba1 occur in a very large crystallographic polyhedron with a complex morphology and a global 13-fold coordination: 11 oxygen atoms are bonded to the atom at the Ba site with an average Ba–O bond length of 2.902 Å, and 12 oxygen atoms are bonded to the atom at the Ba1 site with an average bond length of 2.948 Å (Table 6; Fig. 4a). The Ca/Ca1 site shows a global eight-fold coordination, with a morphology corresponding to a very distorted cube (Fig. 4b), but each individual Ca atom is bonded to seven oxygen atoms, with average Ca–O and Ca1–O bond lengths of 2.461 and 2.490 Å, respectively (Table 6). The Ca2 atom is bonded to the pair of OW1A/OW1B oxygen atoms resulting from the splitting of OW1, thus leading to an eight-fold coordination. However, the Ca2 coordination polyhedron shows a morphology close to that of a seven-fold very distorted pentagonal bipyramid, with an average Ca2–O bond length of 2.406 Å (Table 6, Fig. 5).

DISCUSSION

Comparison between the frameworks of limousinite and phillipsite-Ca

Limousinite is the fourth natural Ba-beryllophosphate known to date, after babefphite [$BaBe(PO_4)F$], minjiangite, and wilancookite. However, the crystal structures of these minerals are completely different: babefphite is triclinic pseudotetragonal and shows a framework containing large ribbons of four tetrahedra

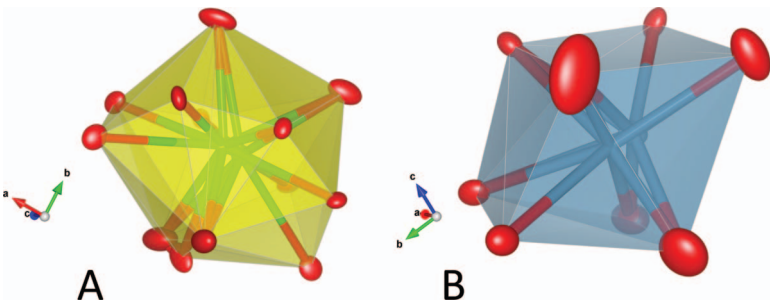

FIG. 4. (A) The $Ba/Ba1O_{13}$ site and (B) the $Ca/Ca1O_8$ distorted cubic site in the crystal structure of limousinite.

TABLE 6. SELECTED BOND DISTANCES (Å) FOR LIMOUSINITE

P1–O4	1.535(4)	P2–O3	1.532(4)	P3–O11	1.520(4)
P1–O8	1.525(4)	P2–O5	1.526(4)	P3–O12	1.527(4)
P1–O9	1.521(4)	P2–O6	1.521(4)	P3–O15	1.530(4)
P1–O2	1.530(4)	P2–O7	1.522(4)	P3–O16	1.522(4)
Mean	1.528	Mean	1.525	Mean	1.525
P4–O1	1.529(4)	Be1–O6	1.634(7)	Be2–O1	1.661(4)
P4–O10	1.537(4)	Be1–O8	1.613(7)	Be2–O4	1.618(7)
P4–O13	1.516(4)	Be1–O11	1.619(7)	Be2–O5	1.601(7)
P4–O14	1.528(4)	Be1–O12	1.603(7)	Be2–O10	1.627(7)
Mean	1.528	Mean	1.617	Mean	1.627
Be3–O9	1.632(7)	Be4–O3	1.625(8)		
Be3–O2	1.641(7)	Be4–O7	1.623(8)		
Be3–O13	1.614(7)	Be4–O14	1.624(7)		
Be3–O15	1.610(7)	Be4–O16	1.597(7)		
Mean	1.624	Mean	1.617		
Ca–OW6	2.125(15)	Ca1–OW6	2.344(8)	Ca2–OW2	2.459(8)
Ca–OW5	2.661(17)	Ca1–OW5	2.396(7)	Ca2–O6	2.479(7)
Ca–OW3	2.751(19)	Ca1–OW3	2.376(7)	Ca2–O7	2.738(8)
Ca–O15	2.86(2)	-	-	Ca2–OW6	1.863(9)
Ca–O4	2.536(15)	Ca1–O4	2.473(5)	Ca2–O12	2.590(8)
-	-	Ca1–O10	2.508(6)	Ca2–OW4	2.244(10)
Ca–O2	2.366(14)	Ca1–O2	2.673(6)	Ca2–OW1A	2.500(16)
Ca–OW4	1.931(18)	Ca1–OW4	2.375(9)	Ca2–OW1B	2.375(16)
Mean	2.461	Mean	2.449	Mean	2.406
Ba–OW2	3.115(10)	Ba1–OW2	2.838(5)		
Ba–OW5	3.032(7)	Ba1–OW5	2.987(6)		
Ba–OW3	2.812(9)	Ba1–OW3	3.093(6)		
Ba–O1	2.573(10)	Ba1–O1	2.941(4)		
Ba–O5	2.817(5)	Ba1–O5	2.797(4)		
Ba–O8	2.799(5)	Ba1–O8	2.788(4)		
Ba–O11	3.200(11)	Ba1–O11	2.828(4)		
Ba–O2	2.869(9)	Ba1–O2	3.222(4)		
Ba–OW1A	2.74(2)	Ba1–OW1A	2.80(3)		
Ba–OW1B	2.88(3)	Ba1–OW1B	2.88(3)		
-	-	Ba1–O16	3.145(5)		
-	-	Ba1–O7	3.062(4)		
Ba–O13	3.084(11)	-	-		
Mean	2.902	Mean	2.948		

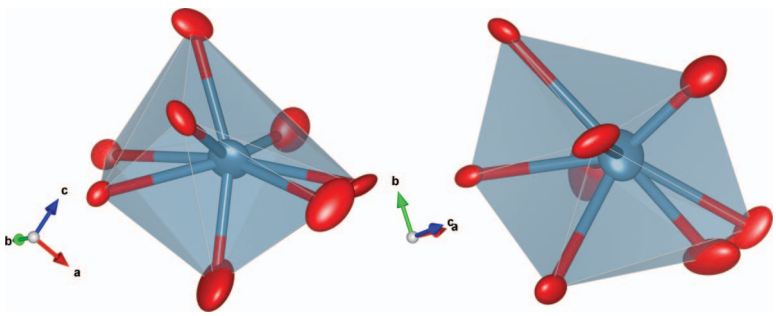

FIG. 5. The $Ca2O_8$ polyhedron in the crystal structure of limousinite, a very distorted pentagonal bipyramid (two different orientations).

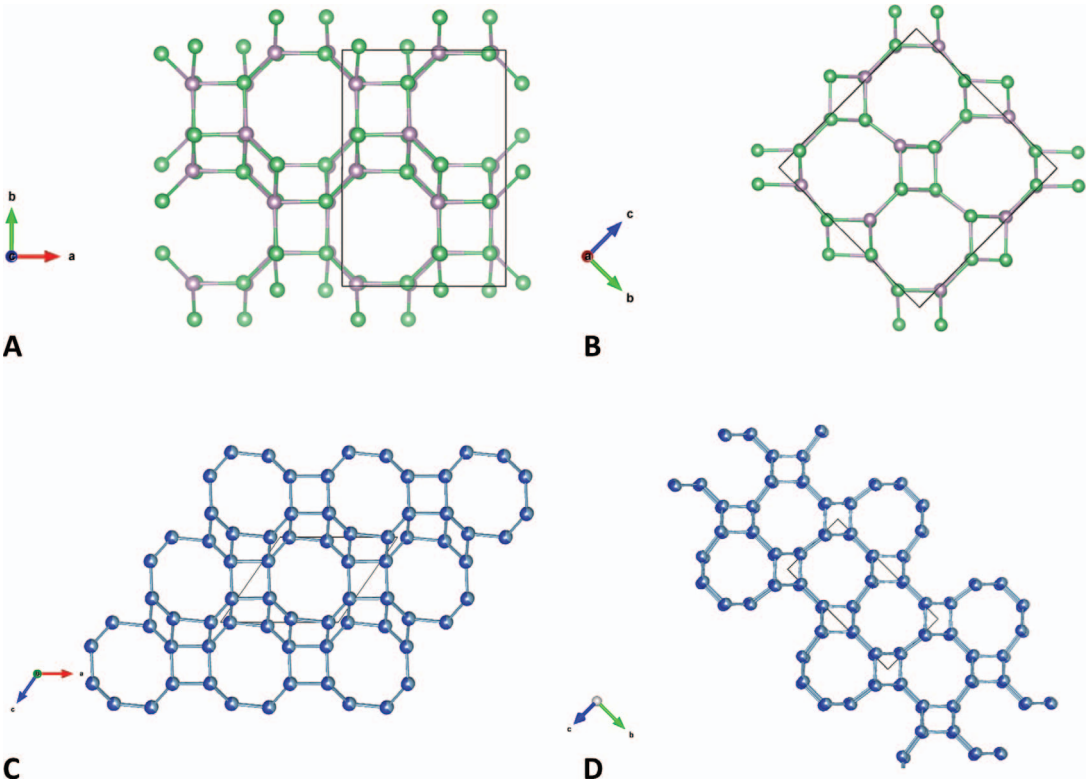

FIG. 6. Comparison between the frameworks of (A, B) limousinite and (C, D) phillipsite-type zeolites.

width (Simonov *et al*. 1980), minjiangite is hexagonal, with a phyllophosphate structure (Rao *et al*. 2015), and wilancookite is cubic, with a zeolite-RHO-type framework (Hatert *et al*. 2017). Limousinite shows a framework topologically identical to that of phillipsite-group zeolites; it is the third zeolite-type phosphate, after pahasapaite (Rouse *et al*. 1987, 1989) and wilancookite (Hatert *et al*. 2017). The mineral can be classified with the Strunz number 08.CA.25, Dana number 40.05.18.01. Table 7 gives a comparison between the properties of limousinite, phillipsite-Ca, minjiangite, wilancookite, and babefphite.

A comparison between the frameworks of limousinite and phillipsite-Ca (Gatta *et al*. 2009) is shown in Figure 6. These identical frameworks are characterized by eight-membered rings, connected with four-membered rings to form cages in which water molecules and large cations (Ca, Ba, K) occur. The diameter of the large eight-membered rings is around 8 Å in limousinite and 10 Å in phillipsite-Ca; this difference is partially due to the shorter P–O (1.52–1.53 Å) and Be–O (1.62–1.63 Å; Table 6) distances in limousinite, compared to the longer *T*–O distances in phillipsite-Ca (1.64–1.67 Å; Gatta *et al*. 2009). The unit-cell settings are also significantly different for the two mineral species, as shown in Figure 6: **a** and **b** have the same orientations, but **c** points in another direction, thus explaining the different β values. Similarities between *a* and *b* are obvious in Table 7, where $a = 9.4958(4)$ and $b = 13.6758(4)$ Å for limousinite, while $a = 9.9238(6)$ and $b = 14.3145(5)$ Å for phillipsite-Ca. The matrix to transform the unit-cell of limousinite to that of phillipsite-Ca is: 1 0 0 / 0 1 0 / –0.5 0 0.5.

Expected exchange behavior of limousinite

Compounds of the zeolite family are extremely important in industry, and solid-state chemists experimentally investigated beryllophosphate systems in order to produce new materials. Synthetic zeolite beryllophosphates are quite common in the literature; they exhibit framework topologies similar to those of gismondine (Coker & Rees 1992, Harrison 2001), analcime (Zhang *et al*. 2003), chabazite (Zhang *et al*. 2002), gmelinite (Zhang *et al*. 2001), or merlinoite (Bu *et al*. 1998), for example.

The crystal chemistry of zeolites is extremely complex due to the partly occupied sites and often

TABLE 7. COMPARISON OF CRYSTAL DATA AND PHYSICAL PROPERTIES OF LIMOUSINITE, PHILLIPSITE-Ca, MINJIANGITE, WILANCOOKITE, AND BABEFPHITE

Mineral Reference	Limousinite This work	Phillipsite-Ca (1, 2)	Minjiangite (3)	Wilancookite (4)	Babefphite (5, 6)
Ideal formula	$BaCa[Be_4P_4O_{16}]\cdot 6H_2O$	$Ca_3[Si_{10}Al_6O_{32}]\cdot 12H_2O$	$Ba[Be_2P_2O_8]$	$(Ba,Li,\square)_8(Ba,Na,K)_6[Be_{24}P_{24}O_{96}]\cdot 26H_2O$	$BaBe(PO_4)F$
Space group	$P2_1/c$	$P2_1/m$	$P6/mmm$	$I23$	$P\bar{1}$
a (Å)	9.4958(4)	9.9238(6)	5.030(8)	13.5398(2)	6.889(3)
b (Å)	13.6758(4)	14.3145(5)	-	-	16.814(7)
c (Å)	13.4696(4)	8.7416(5)	7.467(2)	-	6.902(3)
β (°)	90.398(3)	124.920(9)	-	-	90.01(3)
Z	4	2	1	2	89.99(3)
Strong X-ray	-	7.140 (100)	-	-	90.32(3)
Lines	-	7.105 (100)	-	-	8
	-	-	-	6.90 (60)	-
	-	6.385 (60)	-	-	-
	-	5.362 (60)	-	5.54 (80)	-
	-	5.036 (60)	-	-	-
	-	4.112 (80)	-	-	-
	-	4.092 (60)	-	-	-
	3.89 (100)	-	-	-	4.63 (50)
	3.75 (60)	-	3.763 (100)	-	4.180 (30)
	-	-	-	3.630 (60)	-
	-	3.254 (80)	-	-	-
	-	3.245 (60)	-	3.212 (70)	-
	-	3.177 (100)	-	-	-
	3.09 (60)	3.099 (1)	-	3.043 (100)	3.672 (60)
	3.01 (90)	2.948 (40)	-	-	-
	-	-	-	2.885 (70)	-
	-	-	2.836 (81)	-	3.190 (100)
	-	2.743 (80)	-	2.774 (80)	-
	-	2.738 (80)	-	-	-
	-	2.690 (80)	-	-	-
	-	2.683 (80)	-	-	-
	-	2.515 (5)	2.515 (32)	-	2.760 (80)
	-	2.392 (5)	-	2.398 (60)	-
	2.219 (50)	2.220 (5)	-	-	-
	-	-	2.178 (26)	-	-
	-	2.162 (1)	2.162 (20)	-	-
	-	2.074 (20)	2.090 (64)	-	2.440 (70)
	2.058 (60)	2.056 (20)	-	-	-

TABLE 7. CONTINUED.

Mineral Reference	Limousinite This work	Phillipsite-Ca (1, 2)	Minjiangite (3)	Wilancookite (4)	Babefphite (5, 6)
	1.897 (40)	-	-	-	-
	-	1.773 (40)	1.770 (16)	-	-
	1.735 (40)	1.723 (40)	-	-	2.163 (100)
	-	-	1.507 (25)	-	2.109 (60)
Cleavage	None	{010} distinct	None	None	2.033 (70)
Density	2.58 (calc.)	2.16(1)	3.49 (calc.)	3.05 (calc.)	1.832 (60)
Hardness	-	4–5	~6	4–5	1.741 (10)
Color	Colorless	Colorless	White	Colorless	1.725 (30)

(1) Galli & Loschi Ghittoni (1972); (2) Gatta *et al.* (2009); (3) Rao *et al.* (2015); (4) Hatert *et al.* (2017); (5) Nazarova *et al.* (1966); (6) Simonov *et al.* (1980).

disordered interstitial constituents (water molecules, large low-charge cations), as well as the variable order-disorder relationships between tetrahedral framework cations (Si/Al in aluminosilicates). The limousinite framework is architecturally equivalent to that of phillipsite-group zeolites, but with an ordered P^{5+} and Be^{2+} distribution in a simple 1:1 stoichiometry (Fig. 6), while the Si:Al ratio departs from 1:1 in phillipsite-group zeolites (Si:Al ratio is 5:3 in phillipsite-Na; Gatta *et. al*. 2009), implying a more complex tetrahedral cation ordering.

In limousinite, every framework O atom is bonded to 1 P and 1 Be atoms with simple Pauling bond strengths of 1.25 and 0.50, respectively. This 1:1 ratio with an ordered arrangement of framework Be and P is well known in beryllophosphates, in which P–O–P or Be–O–Be bridges are forbidden because they would lead to bridging O atoms that are either oversaturated ($1.25 + 1.25 = 2.50$) or undersaturated ($0.5 + 0.5 = 1.00$). As all P–O and Be–O individual bonds are near their respective mean <T–O> values (Table 6), we can infer that every framework O atom must have a significant bonding interaction with an interstitial constituent (interstitial cation or H-bond), so that the overall bond-valence requirements of the framework O atoms are satisfied (*i.e.*, $1.25 + 0.50 + 0.25$). This is fundamentally different from aluminosilicate zeolites, in which a significant number of framework O atoms experience Si–O–Si environments where these O-atoms do not require any significant bonding contribution from a neighboring interstitial constituent.

As a consequence, the limousinite framework should possess an overall "more needy" bonding affiliation with its interstitial constituents (*i.e.*, all framework O atoms in limousinite are underbonded from the P–Be contributions alone), implying modifications in the exchange properties of this zeolite compared to those of phillipsite-group zeolites. This feature was described by Coker & Rees (1992), who underlined that the electrostatic field strength in beryllophosphate frameworks is much greater than in the corresponding aluminosilicates. Consequently, the channel mobility within limousinite should be hampered by its framework O bond-valence deficiency, relative to that of phillipsite-Na with an Si:Al ratio of 5:3. This framework difference between limousinite and phillipsite-group zeolites is an independent variable influencing exchange behavior, separate from channel size effects.

The ideal formula of wilancookite

Hatert *et al*. (2017) described the new mineral species wilancookite, a barium beryllophosphate with a zeolite-RHO framework. A careful look at the data

published by these authors indicated some inconsistencies between the structural data and the simplified chemical formula of wilancookite, given as (Ba,K,Na)$_8$(Ba,Li,□)$_6$Be$_{24}$P$_{24}$O$_{96}$·32H$_2$O.

The wilancookite structure was refined in space group *I*23 and the Ba1 site was reported to have a refined occupancy of 0.967(8)Ba + 0.033(8)□, while the Ba2 site showed a refined occupancy of 0.532(6)Ba + 0.468(6)□. In the refinement procedure, the Ba1 site showed a relatively higher site-scattering value of 54.15 electrons compared to the Ba2 site, which showed a site-scattering value of 29.79 electrons. The authors consequently distributed the cations as follows: (Ba$_{7.54}$K$_{0.32}$Na$_{0.14}$)$_{\Sigma 8.00}$ at the "heavy" Ba1 site and (Ba$_{3.04}$Li$_{1.57}$□$_{1.39}$)$_{\Sigma 6.00}$ at the "light" Ba2 site.

The problem with the above expression is that the "heavy" Ba1 site is actually located at the 6*b* Wyckoff position and the "light" Ba2 site is located at the 8*c* Wyckoff position, thus the interstitial cation content between the two Ba sites requires reassessment and formula restructuring. A simple re-organization of the same constituents in a manner conformable with the correct respective Ba-site multiplicities gives (Ba$_{5.04}$Li$_{1.57}$□$_{1.39}$)$_{\Sigma 8.00}$(Ba$_{5.54}$K$_{0.32}$Na$_{0.14}$)$_{\Sigma 6.00}$. According to this cation distribution, the calculated site-scattering values are 52.97 electrons for the Ba1 site and 35.86 electrons for the Ba2 site; these values are in fairly good agreement with the refined site-scattering values given above.

The H$_2$O content in the wilancookite formula is 32 H$_2$O *pfu*, a value which is entirely based upon the structure refinement. According to the data published by Hatert *et al*. (2017), two sites host the H$_2$O molecules: the W1 site located at a 24*f* Wyckoff position and the W2 site at the 2*a* position. Both sites are fully occupied, giving a total of 26H$_2$O *pfu*, which is considerably less than the 32H$_2$O presented in the formula.

As a consequence, we recommend modifying the empirical formula of wilancookite as follows: (Ba$_{5.04}$Li$_{1.57}$□$_{1.39}$)$_{\Sigma 8.00}$(Ba$_{5.54}$K$_{0.32}$Na$_{0.14}$)$_{\Sigma 6.00}$Be$_{24}$P$_{24}$O$_{96}$·26H$_2$O. The simplified formula becomes (Ba,Li,□)$_8$(Ba,K,Na)$_6$Be$_{24}$P$_{24}$O$_{96}$·26H$_2$O and the idealized formula becomes (Ba$_5$Li$_2$□)Ba$_6$Be$_{24}$P$_{24}$O$_{96}$·26H$_2$O. This modification does not need to pass through the CNMNC, since it does not involve an addition or subtraction of significant chemical elements (Nickel & Grice 1998).

Acknowledgments

The authors thank Guest Editor E. Roda Robles for handling the manuscript, as well as I.V. Pekov and M. Cooper for their constructive comments that helped to substantially improve this paper.

References

Alluaud, F. (1826) Notices sur l'hétérosite, l'hureaulite (fer et manganèse phosphatés), et sur quelques autres minéraux du département de la Haute-Vienne. *Annales des Sciences Naturelles* **8**, 334–354.

Bu, X., Gier, T.E., & Stucky, G.D. (1998) Hydrothermal synthesis and low temperature crystal structure of an ammonium beryllophosphate with the merlinoite topology. *Microporous and Mesoporous Materials* **26**, 61–66.

Burnham, C.W. (1991) *LCLSQ version 8.4, least-squares refinement of crystallographic lattice parameters*. Department of Earth & Planetary Sciences, Harvard University, Cambridge, Massachusetts, United States, 24 pp.

Coker, E.N. & Rees, L.V.C. (1992) Ion exchange in beryllophosphate-G. Part 1. Ion exchange equilibria. *Journal of the Chemical Society – Faraday Transactions* **88**, 263–272.

Damour, A. (1847) Sur un nouveau minéral composé de phosphate de fer, de manganèse et de soude, trouvé dans le département de la Haute-Vienne. *Comptes Rendus hebdomadaires des Séances de l'Académie des Sciences* **25**, 670–671.

Damour, A. (1848) Sur un nouveau phosphate de fer, de manganèse et de soude, l'alluaudite, trouvé dans le département de la Haute-Vienne. *Annales des mines* **13**, 341–350.

Delamarre, X. (2003) *Dictionnaire de la langue gauloise. Une approche linguistique du vieux-celtique continental*. Errance Ed., Paris, France, 440 pp.

Fransolet, A.-M. (1975) *Etude minéralogique et pétrologique des phosphates de pegmatites granitiques*. Unpublished Ph.D. Thesis, University of Liège, Belgium, 333 pp.

Galli, E. & Loschi Ghittoni, A.G. (1972) The crystal chemistry of phillipsites. *American Mineralogist* **57**, 1125–1145.

Gatta, D., Cappelletti, P., Rotiroti, N., Slebodnick, C., & Rinaldi, R. (2009) New insights into the crystal structure and crystal chemistry of the zeolite phillipsite. *American Mineralogist* **94**, 190–199.

Harrison, W.T.A. (2001) [H$_3$N(CH$_2$)$_2$NH$_3$]$_{0.5}$[BePO$_4$], a beryllophosphate analogue of aluminosilicate zeolite gismondine. *Acta Crystallographica* **C57**, 891–892.

Hatert, F. (2019) A new nomenclature scheme for the alluaudite supergroup. *European Journal of Mineralogy* **31**, 807–822.

Hatert, F., Philippo, S., Ottolini, L., Dal Bo, F., Scholz, R., Chaves, M.L.S.C., Yang, H., Downs, R.T., & Menezes Filho, L.A.D. (2017) Wilancookite, (Ba,K,Na)$_8$(Ba,Li,□)$_6$Be$_{24}$P$_{24}$O$_{96}$·32H$_2$O, a new beryllophosphate with a zeolite framework. *European Journal of Mineralogy* **29**, 923–930.

HAUSMANN, J.F.L. (1813) Triplit. *In* Handbuch der Mineralogie – Volume 2. Göttingen, Germany, 1079–1080.

KRAUZ, W. & NOLZE, G. (1996) *POWDER CELL* – A program for the representation and manipulation of crystal structures and calculation of the resulting X-ray powder patterns. *Journal of Applied Crystallography* **29**, 301–303.

LEBOCEY, J., MEISSER, N., CHATENET, F.X., BOISSON, J.M., & HUSSON, F. (2010) Découverte d'arthurite dans les Monts d'Ambazac (Haute-Vienne). *Le Règne minéral* **96**, 51.

MANDARINO, J.A. (1981) The Gladstone-Dale relationship: Part IV. The compatibility concept and its application. *Canadian Mineralogist* **19**, 441–450.

MEISSER, N. (2010) Sur la présence de bendadaite à la Vilatte-Haute (Monts d'Ambazac, Haute-Vienne). *Le Règne minéral* **94**, 40.

MEISSER, N., CHATENET, F.X., & LEBOCEY, J. (2009) Nouvelles observations sur la minéralogie des pegmatites à phosphates de la région de Chanteloube, Haute-Vienne. *Le Règne minéral*, *hors série* **14**, 64–66.

MOORE, P.B. & ITO, J. (1979) Alluaudites, wyllieites, arrojadites: Crystal chemistry and nomenclature. *Mineralogical Magazine* **43**, 227–235.

NAZAROVA, A.S., KUZNETSOVA, N.N., & SHASKIN, D.P. (1966) Babefphite, a barium beryllium fluoride-phosphate. *Doklady Akademii Nauk SSSR* **167**, 895–897.

NICKEL, E.H. & GRICE, J.D. (1998) The IMA Commission on New Minerals and Mineral Names: Procedures and guidelines on mineral nomenclature. *Canadian Mineralogist* **36**, 10–20.

OXFORD DIFFRACTION (2007) *CrysAlis CCD* and CrysAlis RED, *version 1.71*. Oxford Diffraction, Oxford, England.

RAO, C., HATERT, F., WANG, R.C., GU, X.P., DAL BO, F., & DONG, C.W. (2015) Minjiangite, $BaBe_2(PO_4)_2$, a new mineral from Nanping No. 31 pegmatite, Fujian Province, southeastern China. *Mineralogical Magazine* **79**, 1195–1202.

ROUSE, R.C., PEACOR, D.R., DUNN, P.J., CAMPBELL, T.J., ROBERTS, W.L., WICKS, F.J., & NEWBURY, D. (1987) Pahasapaite, a beryllophosphate zeolite related to synthetic zeolite rho, from the Tip Top pegmatite of South Dakota. *Neues Jahrbuch für Mineralogie Monatshefte* **1987**, 433–440.

ROUSE, R.C., PEACOR, D.R., & MERLINO, S. (1989) Crystal structure of pahasapaite, a beryllophosphate mineral with a distorted zeolite rho framework. *American Mineralogist* **74**, 1195–1202.

SIMONOV, M.A., EGOROV-TISMENKO, Y.K., & BELOV, N.V. (1980) Use of modern X-ray equipment to solve fine problems of structural mineralogy by the example of the crystal structure of babefphite $BaBe(PO_4)F$. *Soviet Physics Crystallography* **25**, 28–31.

VAUQUELIN, N. (1802) Sur un phosphate natif de fer mélangé de manganèse. *Journal des mines* **11**, 295–300.

WILSON, A.J.C. (1992) *International Tables for X-ray Crystallography, Vol. C*. Kluwer Academic Press, London, England, 883 pp.

ZHANG, H., CHEN, M., SHI, Z., BU, X., ZHOU, Y., XU, X., & ZHAO, D. (2001) Hydrothermal synthesis of new pure beryllophosphate molecular sieve phases from concentrated amines. *Chemistry of Materials* **13**, 2042–2048.

ZHANG, H., WENG, L., ZHOU, Y., CHEN, Z., SUN, J., & ZHAO, D. (2002) $[C_6N_4H_{24}]CoBe_6P_6O_{24}{\cdot}3H_2O$: A novel 3-dimensional beryllophosphate zeolite-like structure encapsulating Co^{II} ions. *Journal of Material Chemistry* **12**, 658–662.

ZHANG, H., CHEN, Z., WENG, L., ZHOU, Y., & ZHAO, D. (2003) Hydrothermal synthesis of new beryllophosphates M^I-BeBPO ($M^I = K^+$, Na^+ and NH_4^+) with zeolite ANA framework topology. *Microporous and Mesoporous Materials* **57**, 309–316.

Received January 31, 2020. Revised manuscript accepted May 22, 2020.